J Mol Model (2002) 8:119–130
DOI 10.1007/s00894-002-0080-2

ORIGINAL PAPER

Marcus Lundberg · Margareta R. A. Blomberg
Per E. M. Siegbahn

Density functional models of the mechanism for decarboxylation in orotidine decarboxylase

Received: 19 November 2001 / Accepted: 11 March 2002 / Published online: 24 April 2002

Abstract The mechanism of orotidine 5-monophosphate decarboxylase (ODCase) has been modeled using hybrid Density Functional Theory (B3LYP functional). The main goal of the present study was to investigate if much larger quantum chemical models of the active site than previously used could shed new light on the mechanism. The models used include the five conserved amino acids expected to be the most important ones for catalysis. One result of this model is that a mechanism involving a direct cleavage of the C–C bond followed by a protonation of C6 by Lys93 appears unlikely, with a barrier for decarboxylation 20 kcal mol^{-1} too high. Additional effects like electrostatic stress and ground-state destabilization have been estimated to have only a minor influence on the reaction barrier. The conclusion from the calculations is that the negative charge developing on the substrate during decarboxylation must be stabilized by a protonation of the carbonyl O2 of the substrate. For this mechanism, the addition of the catalytic amino acids decreases the reaction barrier by 25 kcal mol^{-1}, but full agreement with experimental results has still not been reached. Further modifications of this mechanism are discussed. Electronic supplementary material to this paper can be obtained by using the Springer LINK server located a http://dx.doi.org/10.1007/s00894-002-0080-2.

Keywords Enzyme catalysis · Density Functional Theory · Orotidine 5'-monophosphate decarboxylase

Introduction

Orotidine 5'-monophosphate decarboxylase (ODCase, 4.1.1.23) catalyzes the decarboxylation of orotidine 5'-monophosphate (OMP) to uridine 5'-monophosphate (UMP) (Fig. 1). [1] This is the sixth and final step in the de novo biosynthesis of UMP, which is a major precursor in the formation of the pyrimidine nucleotides cytosine, C and thymine, T. ODCase increases the rate of decarboxylation by 17 orders of magnitude, [2] thus showing a remarkable catalytic proficiency. In addition to its proficiency, the enzyme is also unique in that the lone-pair of the carbanion generated by loss of carbon dioxide is localized in an sp^2 orbital of the σ-system of the pyrimidine ring. In other known decarboxylations, the electron pair remaining after breakage of the carbon–carbon bond can be stabilized by delocalization either into a π orbital or by a covalently attached cofactor. ODCase contains no cofactor or metal ion. [3, 4, 5]

Kinetic studies have shown that decarboxylation occurs in the enzyme at a rate of tens of turnovers per second. [3, 6, 7, 8] Transition State Theory gives a free energy barrier of 15 kcal mol^{-1} for a reaction rate of 14 s^{-1}. k_{cat}/K_m is around 1.65×10^7 M^{-1} s^{-1}. [8] An Arrhenius plot of the enzymatic reaction kinetics gives an enthalpy of activation $\Delta H^{\ddagger}$ z of 11 kcal mol^{-1}. [9] $T\Delta S^{\ddagger}$ is then approximately –4 kcal mol^{-1} at room temperature.

Porter and Short found [8], in agreement with previous studies [10] that the enzyme kinetics is governed by two

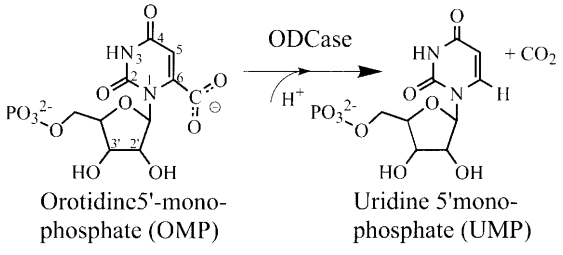

Fig. 1 Reaction catalyzed by ODCase

Electronic supplementary material to this paper can be obtained by using the Springer LINK server located a http://dx.doi.org/10.1007/s00894-002-0080-2.

M. Lundberg (✉) · M.R.A. Blomberg · P.E.M. Siegbahn
Department of Physics, Stockholm Center for Physics, Astronomy and Biotechnology, Stockholm University, 106 91 Stockholm, Sweden
e-mail: marc@physto.se

ionizations (e.g. proton transfers). The first at pH=6.1 (for OMP) depends on substrate and is argued to be a complex function of ionizations in the purinyl ring and the phosphate group. The second at pH=7.7 is attributed to an interacting group on the enzyme. They also found that the enzyme removes a proton from the solvent when the product is released. The rate of the catalyzed reaction is not exceptional, it is the slowness of the uncatalyzed reaction that leads to the large rate increase in ODCase. In a physiological buffer, the substrate has a half-life of 78 million years. The uncatalyzed reaction has an enthalpy of activation $\Delta H^{\ddagger}$=44 kcal mol^{-1} (derived from an Arrhenius plot). The entropy of activation ($T\Delta S^{\ddagger}$) is +6 kcal mol^{-1}, [2] which is in the opposite direction compared to the enzymatic reaction.

Several proposals have been put forward in attempts to explain the catalyzing power of ODCase. An early suggestion was a covalent mechanism involving a nucleophilic attack on C5 of the substrate [11] (for the numbering of the atoms, see Fig. 1). However, NMR data, [12] kinetic isotope effects [10, 12] and inhibitor studies [3] did not support a covalent mechanism.

Beak and Siegel [13] proposed a protonation of a carbonyl oxygen (O2) to form a zwitterion that would stabilize the negative charge developing on C6. Such a mechanism, referred to as the O2 mechanism, appears consistent with the experiments discussed above. [3, 10, 12] Experiments with 2-thioOMP (where O2 has been substituted by S) show that this compound is not a substrate, [3] while at the same time the corresponding product, 2-thioUMP, is a mixed inhibitor of the active site. [14] These observations have been explained by a severely decreased binding affinity for the substituted substrate. [15] There is no direct evidence of O2 involvement in the catalytic reaction, but the results described above imply that O2 has an important role, either in substrate binding or in both binding and catalysis. On the other hand, reactions with 4-thioOMP proceed without significant decrease in rate, [3] which is a strong argument against decarboxylation via a protonated O4 intermediate.

The O2 mechanism was favored until Lee and Houk, [16] on the basis of quantum mechanical calculations on the substrate, showed that protonation of O4 is more favorable than protonation of O2. Later calculations [17] showed that O4 protonation does not give a viable decarboxylation mechanism, having a barrier of 34 kcal mol^{-1}. At the same time the barrier for decarboxylation via protonated O2 was shown to be even higher, 51 kcal mol^{-1}, and these calculations therefore seemed to rule out both the O2 and the O4 mechanisms. Four different X-ray structures with different inhibitors have been published. [18, 19, 20, 21] In these structures, there are no obvious proton donors close to O2 or O4. The Lys93 (yeast enzyme numbering) that was earlier shown to be essential for catalysis [22] is located in a perfect position to stabilize negative charge developing on C6 and to donate a proton to this atom during the reaction. Lys93 is, together with Lys59, Asp91 and Asp96, part of a charged network that

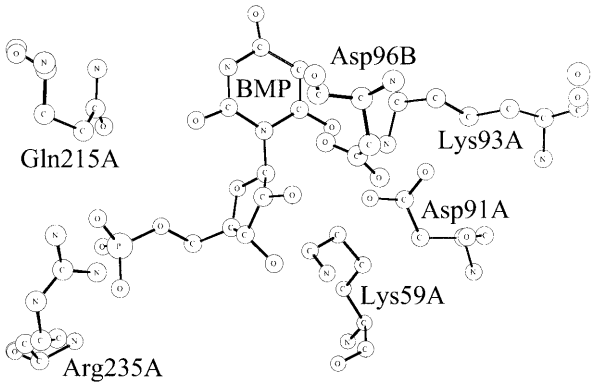

Fig. 2 X-ray structure of ODCase with a bound inhibitor (BMP). Only selected amino acids are shown. A and B denote different subunits

is invariant in all species. [23] Asp96 forms a hydrogen bond to 2'OH of the ribose ring and Lys59 binds to 3'OH (Fig. 2). Substitutions of any of these four charged amino acids for alanine give undetectable activity, except for the L59A mutant enzyme, where k_{cat} is reduced by a factor of 130. [24]

Other invariant amino acids at the active site are Gln215 (hydrogen bonding to O2 and phosphate), Arg235 (hydrogen bonding to phosphate), Asp37 (hydrogen bonding to 3'OH) and Thr100 (hydrogen bonding to 2'OH). [23] Mutation studies have shown that Q215A does not affect the reaction kinetics [24] while the mutations R235A, D37A and T100A have a significant effect on both K_m and k_{cat}. [25, 26]

The interactions with the phosphate group are interesting since Miller et al. have shown that k_{cat} decreases by 5 orders of magnitude for orotidine (without the phosphate group) compared to orotidine 5'P. k_{cat}/K_m decreases by seven orders of magnitude. [27] The contribution to the binding affinity generated by the phosphate group changes with substrate. It is largest for the proposed TS analogue BMP (6-hydroxyuridine 5'phosphate). [28] This implies that the phosphate group assists in the differential binding of reactant and transition state.

The appearance of X-ray structures triggered new mechanistic proposals. None of the structures were crystallized with a carboxylated substrate so the position of the carboxylate group is not well determined. By addition of a carboxylate group to C6 of the BMP inhibitor, this negative group comes within 2.4 Å of the negatively charged Asp91. [21] This observation made three groups suggest that the enzyme works by electrostatic destabilization of the reactant. [18, 20, 21] The repulsion between carboxylate and Asp91 should then be relieved by a decarboxylation that transfers negative charge to C6. Wu et al. [20] also carried out QM/MM calculations and claim that substrate destabilization is the significant catalytic effect. Ground state destabilization has also been proposed previously by other groups. [16, 29]

Warshel and Florián argue against ground state destabilization on general grounds. [30] For an enzyme working

in subsaturating conditions, a ground state destabilization would not increase k_{cat}/K_m, which is the important kinetic factor for an enzyme. Specifically for ODCase, Warshel et al. claim that calculations with the EVB method show that the effect of ground state destabilization is not very important. [31] On the basis of the calculations they suggest a mechanism where C6 is protonated directly by Lys93, and that the important catalytic effect comes from a reduction of the protein–protein reorganization energy.

Different studies of kinetic isotope effects have been made, trying to resolve the mechanistic questions of ODCase. Smiley et al. studied ^{13}C kinetic isotope effects and found that decarboxylation is at least partly rate determining. [10] Using ^{13}C and deuterium solvent studies, Ehrlich et al. found evidence for a stepwise mechanism where a protonation step precedes decarboxylation. [32] This first protonation step could involve O2 and be the first of the two ionizations that Porter and Short observed. [8] It has, however, been argued that the observed isotope effect could arise from substrate binding or from protein conformational changes rather than O2 protonation. [18, 33] Rishavy and Cleland carried out studies with $^{15}N1$ and compared the kinetic isotope effects for orotidine 5'-monophosphate with those for *N*-methyl picolinic acid. Their conclusion is that no bond order change occurs at N1 during the reaction, [33] which seems to be required in the O2 mechanism. However, in a recent paper, Phillips and Lee show, using computational methods, that the $^{15}N1$ kinetic isotope effect is consistent with both O2 and O4 protonation. [34]

In summary, there is no general agreement regarding the mechanism of ODCase. Experimental results alone cannot at this stage determine the reaction mechanism. Important contributions can be made from further computational studies. The main purpose of the present study is to investigate whether larger quantum mechanical models can resolve some of the issues concerning the mechanism. Previous studies have indicated a particularly important role for the charged aspartate and lysine groups at the active site, but so far no theoretical study has incorporated these into the quantum chemical part of the model. As it turns out, the present calculations do not support the direct protonation mechanism involving an electrostatic stabilization of the transition state suggested previously. Therefore, the alternative O2 and O4 mechanisms were also reinvestigated, using larger models than in previous studies, and also incorporating information from the X-ray structures that appeared after the previous studies.

Computational details

All calculations are performed using the DFT hybrid functional B3LYP [35, 36] as implemented in Gaussian98. [37] The calculations are done in several steps. Geometries are first optimized using the d95 basis set, which is a double zeta basis set. [38] The same basis set is used also for the Hessian calculations, i.e. second derivatives of the energy with respect to the nuclear coordinates. Optimized structures are accepted if the Hessian only has positive eigenvalues. The Hessians are also used to estimate zero-point, thermal and entropy effects on the relative energies, applying the harmonic approximation. If not stated otherwise, the results in the paper are free energies, which include corrections for solvent and thermal effects.

Transition states (TS) are obtained by full optimizations. The energy surface close to the TS is investigated by scanning one or more bond distances. The Hessian from a reasonable guess structure is used to locate the TS. TSs are characterized by a single negative eigenvalue in the Hessian. In one of the reaction models, there is no energy barrier on the energy surface and a barrier can only be found by separately adding the entropy contribution. The free energy of the reaction has then been studied by freezing the reaction coordinate at different points between reactant and product.

Following the geometry optimization, the energy is calculated using d95+(2d,2p), with polarization functions added to all atoms and diffuse functions added to the heavy atoms. Optimizing with a small basis set is sufficient since the final energy is rather insensitive to the quality of the geometry optimization. [39] To check the influence of the choice of basis set in the optimization, a reaction barrier was calculated following optimization with the 6-31G(d,p) basis set. Only a minor change in the barrier height (–0.3 kcal mol^{-1}) was found. The inherent accuracy of the B3LYP method has been estimated using the extended G3 benchmark set. [40] Excluding the set of 75 enthalpies of formation for large molecules, which are not very relevant when studying reaction mechanisms where only a few bonds are formed or broken, the B3LYP functional has an error of 3.29 kcal mol^{-1} (301 entries). To estimate the accuracy of the calculated B3LYP barriers for the present system, accurate G2MS calculations [41] were performed on two small models. G2MS calculations gives a 4 kcal mol^{-1} higher barrier for a TS involving proton transfer (direct protonation mechanism below) but only a 1 kcal mol^{-1} higher barrier for unconcerted cleavage of the C6-carboxylate bond (O2 mechanism).

The part of the protein that is not explicitly included in the model is treated as a homogenous medium with a dielectric constant of 4. Corrections for solvent effects are calculated using the CPCM polarizable conductor model (Cosmo). [42, 43] The radii of the solvent molecules are taken from the parameters for water.

As further described below, several different models of the active site are used in the calculations. The substrate orotidine is generally modeled as deprotonated 1-methylorotorate. In some calculations, parts of the ribose ring have been added. Lysine residues are modeled by methylamine while methylamide has been used for glutamine. Aspartates are generally modeled as formate ions.

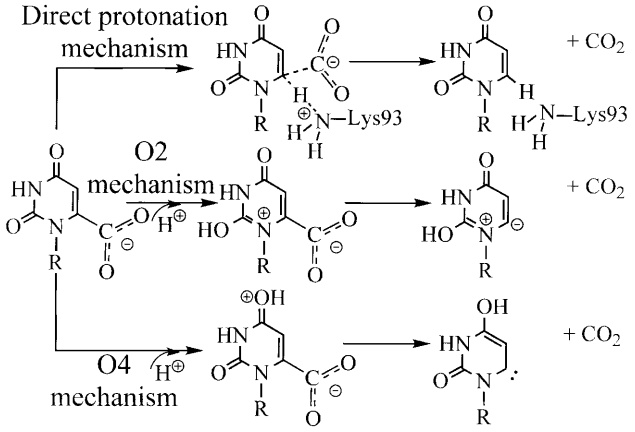

Fig. 3 Schematic drawing of the three major reaction mechanisms proposed for ODCase. Note that the O2 and O4 mechanisms require a shift of a proton from the hydroxyl group to C6 in order to complete the reaction

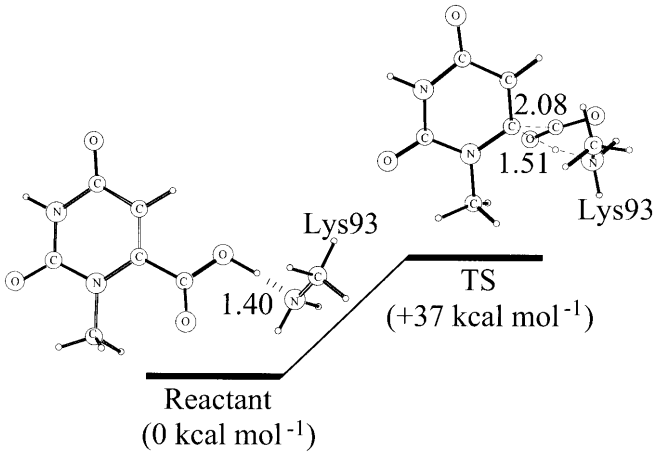

Fig. 4 Reactant and TS in the simple model with Lys93 (Model 1). The number 1.40 is the N–H bond distance (in Å) in the reactant. The numbers 2.08 and 1.51 are the C–C and C–H bond distances (in Å) at the TS

Results

Three major groups of reaction mechanisms have been proposed for ODCase as illustrated in Fig. 3. The upper mechanism is the one (with different modifications) that is at present favored by most researchers in the field. [20, 21, 44, 45] In this mechanism, which will be termed the direct protonation mechanism, Lys93 donates a proton to C6 of the orotidine ring concerted with (or after) cleavage of the C–C bond between the ring and the carboxylate. In the second major group of mechanisms, the middle one in Fig. 3, a key step is a protonation of O2 of the orotidine ring which triggers the loss of the carboxylate at the C6 position. This mechanism will be termed the O2 mechanism. Finally, in the third group of mechanisms, the lower one in Fig. 3, protonation of O4 leads to the loss of the carboxylate. The O4 mechanism appears to be the one used in the uncatalyzed reaction. [17] Experiments indicate that this mechanism is less likely for the enzyme. [3] A summary of the most important models used in the present study is shown in Table 1.

The direct protonation reaction mechanism

A large number of models, differing in size and charge, were used to study the direct protonation mechanism, shown uppermost in Fig. 3. In the first and simplest model (Model 1 in Table 1), only the deprotonated substrate and the protonated Lys93 were included, see Fig. 4. The calculated barrier for this model is as high as 37 kcal mol^{-1}, rather close to the uncatalyzed reaction with 38 kcal mol^{-1}, [2] and much higher than the experimental value of 15 kcal mol^{-1} for the enzyme. In the gas phase optimization, lysine donates its proton to the carboxylate in the reactant. If the structures are optimized in a low-dielectric medium, the substrate stays negatively charged and the barrier decreases by 2 kcal mol^{-1} to 35 kcal mol^{-1}. For more elaborate models the effect of the surrounding would probably be smaller. The result from the gas phase optimization (37 kcal mol^{-1}) agrees well with that obtained for a similar model by Warshel et al. [31] (around 38 kcal mol^{-1}).

In this simple model, the strong interaction in the reactant between Lys93 and the carboxylate group is one reason for the large barrier. When carbon dioxide is formed in the product, this interaction energy will be essentially zero. One way to decrease this attractive interaction in the reactant is to add the nearest negative aspartate (Asp91) to the model (Model 2). Indeed, this leads to a weaker electrostatic attraction between the carboxylate and the lysine with a hydrogen bond in the reactant being weaker (the bond length increases from 1.4 Å without the aspartate to 1.7 Å), but there is only a minor effect on the reaction barrier (–2 kcal mol^{-1}).

In the next set of models, the conserved amino acids Lys59 and Asp96 were added in different steps and in different configurations but no TS lower than 35 kcal mol^{-1} could be found.

One problem with the above models was to correctly describe the hydrogen bonding pattern. The specific arrangement of the charged network might be an important feature of the enzyme. It is known from the X-ray structure that Lys59 and Asp96 have hydrogen bonds to 3'OH and 2'OH of the ribose ring, respectively. To obtain a stable charged network, a new model was designed where 2'OH and 3'OH in the ribose ring were included together with the four conserved amino acids (Model 3). A starting geometry for this optimization was constructed using the coordinates from the pdb-file 1DQX. [19] There is no structure available with the substrate present, so the carboxylate group was simply added to the BMP (6-hydroxyuridine 5'phosphate) inhibitor in this pdb-structure. It is in such an unoptimized structure that the carboxylate comes very close to Asp91, causing some authors to propose a destabilization mechanism. [18, 20, 21] In order to keep the general structure from the X-ray, an initial optimization with restrictions was performed.

Table 1 Summary of model size and $\Delta G^{\ddagger}$ for the most important models

Model	Amino acids	Charge	$\Delta G^{\ddagger}$ (kcal mol^{-1})	Comments
Direct protonation mechanism				
1	Lys93	Neutral	+37	
2	Asp91, Lys93	–1	+35	
3	Lys59, Asp91, Lys93, Asp96	–1	+35	2'- and 3'-OH included
4a	Lys93, Asp, water	Neutral	+32	Hydrogen bond to O2
4b	Lys93, Asp, water	Neutral	+31	Hydrogen bond to O4
5	Asp91, Lys93	Neutral	+45	Substrate protonated
O2 mechanism				
6	No amino acids	Neutral	+50	Substrate protonated
7	Lys59, Asp91, Lys93, Asp96	Neutral	+42	Substrate protonated, 2'- and 3'-OH included
8	Lys59, Asp91, Lys93, Asp96, Gln215, water	Neutral	+26	Substrate protonated, 2'- and 3'-OH included
9	Lys93, Gln215, water	+1	+37	O2 protonated, concerted TS
O4 mechanism				
10	Lys59, Asp91, Lys93, Asp96	Neutral	50 (small basis)	Substrate protonated, 2'- and 3'-OH included

The outer carbon atoms on the amino acid models were frozen with respect to each other, to an atom in the orotidine ring (N3 hydrogen) and to 3'C of the ribose. To get a similar flexibility for the lysine and aspartate residues, aspartate is modeled as acetate instead of formate in this extended model. The restrictions were then released to find a fully optimized minimum (Fig. 5). A fully optimized TS structure was found using the methods described in the computational section. The calculated barrier for this reaction is 35 kcal mol^{-1}, which is much higher than the experimental value of 15 kcal mol^{-1}. Indeed, there is almost no difference between the result of this extended model, including all the nearest conserved and charged amino acids, compared to the results for the simplest model with only one lysine (Model 1). In spite of the large variations in the models used, the barrier is thus remarkably stable.

Before proceeding to other models, a few remarks can be made on the TS structure in Fig. 5. It can, for example, be noted that the C–C bond is stretched to 2.88 Å when the proton is transferred. This is in contradiction with the interpretation of kinetic isotope effects made by Singleton et al. who state that in the catalyzed process in the enzyme the CO_2 loss should occur earlier than in the uncatalyzed reaction (where it is estimated to occur at 2.4 Å). [17] The energy of the TS shows that Lys93 does not significantly affect the C–C bond stretch in this TS. When comparing with the 1-methylorotorate substrate only, the energy cost to stretch the C–C bond to 2.88 Å, is the same as for Model 3.

As the conserved charged network did not have a significant stabilizing effect on the TS in the investigated models, other effects were sought. A viable alternative for stabilizing the negative charge on the substrate is to provide protons to the carbonyl oxygens as previously suggested. [13, 16] Hydrogen bonds to either O2 or O4 would also improve the situation since they would be stronger in the TS compared to the reactant. A single

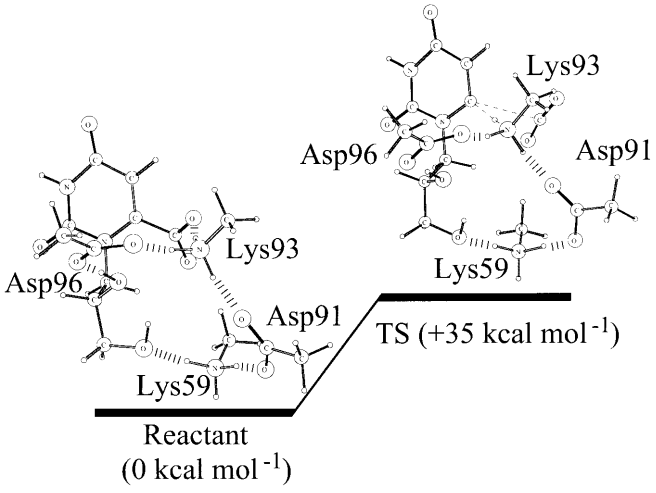

Fig. 5 Reactant and TS for the extended model with an intact charged network with Lys59, Asp91, Lys93 and Asp96 (Model 3). At the TS the C–C bond is 2.88 Å and the C–H bond is 1.76 Å

hydrogen bond to a glutamine or a protonated aspartate did not lower the barrier by more than 1 kcal mol^{-1}. The most significant effect was obtained by forming hydrogen bonded chains between Lys93 and O2 (Model 4a) or O4 (Model 4b), via an aspartate (formic acid) and one water (Fig. 6), which lowered the barrier by up to 6 kcal mol^{-1}. However, this arrangement does not correspond to the X-ray structure, but can be taken as an upper limit for this type of effect.

Harris et al. suggested that the assumed proximity between two negative groups could make them a probable site for protonation. [21] A very strong hydrogen bond would then be formed between carboxylate and Asp91, which is argued to assist in catalysis. Since the UMP product has one extra proton compared to the OMP reactant, it is obvious that this extra proton has to be supplied to the active site during the catalytic cycle. At

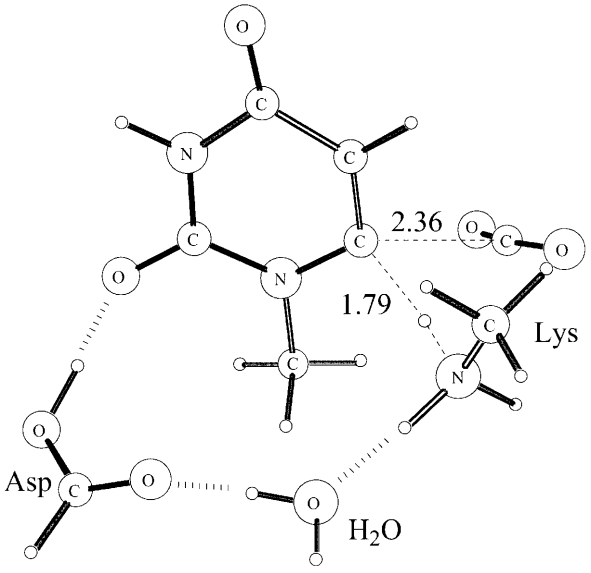

Fig. 6 TS for a model with a hydrogen bonding link to O2 (Model 4a). Numbers represent bond distances in Å

first it seems reasonable that the negative charge developing on C6 would be stabilized if the extra proton is available at the TS. To investigate this possibility a neutral model with a protonated substrate, one protonated lysine and one deprotonated aspartate was used (Model 5). The addition of a proton turned out to increase the barrier for decarboxylation by 8 kcal mol^{-1}, which is opposite to the suggestion made. The increase of the barrier is interpreted as the cost to break two strong hydrogen bonds in the reactant, between carboxylate–Asp91 and between carboxylate–Lys93. Several other positively charged models were tried but none showed a reaction barrier lower than 37 kcal mol^{-1}. The results indicate that protonation of the active site impedes the decarboxylation reaction.

In conclusion, a large number of models of the direct protonation reaction mechanism, where C6 is protonated by Lys93, have been studied. In the largest model, all the amino acids in the charged network on the carboxylate side (Lys59, Asp91, Lys93 and Asp96) were included in the correct hydrogen bonding configuration. However, even in this model a much too high reaction barrier of 35 kcal mol^{-1} was found. In the modeling of this reaction, it furthermore seems that the conserved charged network has no significant effect on the reaction barrier, which is a quite astonishing result. The lowest barrier found for this mechanism is 31 kcal mol^{-1}, including strong hydrogen bonding chains from Lys93 to O2 or O4, but these chains have no support from the X-ray structure. The conclusion drawn at this stage is that the true reaction probably differs significantly from the models described above.

Electrostatic stress and geometric strain

The present results for the direct protonation mechanism disagree with results from previous calculations by Warshel et al. [31] The final barrier obtained for the direct protonation mechanism in the present calculations is too high, 35 kcal mol^{-1}, while the lowest barrier obtained by Warshel et al. is only 19 kcal mol^{-1}, in reasonable agreement with the experimental value of 15 kcal mol^{-1}. The barrier calculated without taking the surrounding protein into account, using an orotidine plus lysine model only, is in fact similar in the two studies, 37–38 kcal mol^{-1}, and therefore the discrepancy between the two investigations seems to come from the treatment of the protein, which indeed is very different. In this section these differences are analyzed.

The major differences between the models used by Warshel et al. and the present Model 3 can be described as follows. In the present model both the substrate and a significant portion of the active site amino acid residues are treated quantum mechanically, while the rest of the protein is described simply as a dielectric medium. In the model used by Warshel et al. only the substrate and one lysine are treated quantum mechanically. On the other hand, the whole protein is described explicitly, although only at a classical level. Furthermore, Warshel et al. argue that the enzyme acts mainly through electrostatic effects, which in their modeling are described by ionizing certain amino acids in the vicinity of the active site. The most important ionized residues are the Asp91 and Asp96, and in a model having only these two amino acids charged (described classically), and using a quantum chemical model including only the orotidine substrate and Lys93, Warshel et al. obtained a barrier of 24 kcal mol^{-1}. A further decrease down to 19 kcal mol^{-1}, in close agreement with the experimental value of 15 kcal mol^{-1}, was obtained by adding additional charged amino acids in their calculations. At this point it should be noted that the main electrostatic effects found by Warshel et al., i.e. from the nearest aspartates, are already taken care of fully quantum mechanically in Model 3, see Fig. 5. Therefore, their result of 24 kcal mol^{-1} for the barrier for a model including only the aspartates as charged residues is very puzzling, since the present calculations give a quantum mechanical value of 35 kcal mol^{-1} for a very similar chemical model.

Several alternatives have been proposed to explain how enzymes decrease reaction barriers, among those are destabilization of the reactant (by protein–substrate interactions), destabilization of the protein in the reactant (accomplished in the folding process) or pure TS stabilization. Destabilization of the reactant (often referred to as the ground state) by the protein as a mechanism for catalysis has been a common suggestion for ODCase. [16, 18, 20, 21, 29] Such a destabilization might be accomplished either by electrostatic effects or by geometric strain. In a first attempt to estimate possible repulsive effects between the substrate and the protein, the proton affinity of the orotidine carboxylate group,

with and without the surrounding enzyme residues was calculated. If there is a significant repulsion between the substrate carboxylate and a negative group in the enzyme (Asp91 for example), the proton affinity of the carboxylate would increase in the enzyme compared to OMP in a water solvent. Several models were used, with and without geometric constraints relative to the X-ray structure, and the largest effect from the protein obtained on the proton affinity is only 6 kcal mol^{-1}, which is not enough to support any significant repulsion between Asp91 and the substrate carboxylate.

The reactant (ground state) destabilization mechanism has previously been criticized by Warshel et al. [31] on a similar basis as discussed above. It was argued that a positive lysine residue located in between negatively charged groups effectively removes large repulsive effects. In addition, if the system were to have a significantly increased proton affinity due to repulsion, a negative group could easily accept a proton from the protein to relieve this repulsion. The reactant (ground state) destabilization mechanism has also been questioned by Miller et al. [24] Their studies of substrate binding in mutated enzymes do not show an increase in binding of OMP in the D91A enzyme where the assumed repulsion has been removed.

The other type of effect for destabilizing the binding of the reactant, geometric strain, is not properly modeled in a free optimization procedure as used here. In general, it is not considered that strain is an important catalytic effect for enzymes, but here an upper limit of such an effect is investigated. The maximal strain effect for decreasing the barrier should be obtained by freezing the amino acids in the positions they have in the TS. If the reactant is bound to the protein with the amino acids totally frozen from the TS structure, the binding energy is lowered by 13 kcal mol^{-1} as compared to the fully optimized structure. Such an extreme strain in the protein cannot occur, of course, but a decrease of the barrier by 13 kcal mol^{-1} is still not enough to give agreement with experiment. A more realistic estimate of a possible strain effect is rather that it is less than 5 kcal mol^{-1}.

Warshel and coworkers argue that, instead of destabilizing the reactant, the enzyme is preorganized to stabilize the TS. [30, 46, 47] In a solvent like water, energy has to be invested to polarize the solvent in the TS, but this is not necessary in the preorganized enzyme. This energy contribution to catalysis comes from interaction between charged enzyme residues, and is termed electrostatic stress by Warshel et al. [31] Their calculations indicate that, if the catalytic effect comes from electrostatic stress in the protein, a large part of this stress should come from the Asp91–Asp96 repulsion, and therefore the issue of electrostatic stress should be possible to investigate using Model 3.

An interesting difference between the present model and the one used by Warshel et al. is that in the present calculations the positions of the selected protein residues are freely optimized for both the ground state and the TS, while in the study by Warshel et al. a relaxed version of the crystal structure is used. The hypothesis of electrostatic stress should have two implications for the present model. First, since the total energy for the TS cannot be lowered by a less optimal structure of the protein, the difference between the results indicates that the reactant has been stabilized too much. The full optimization, as in the present study, could give a reactant structure with too small an electrostatic repulsion, i.e. too low in energy, resulting in the too high barrier. Second, if the enzyme is preorganized for the TS, the present fully optimized TS model should give a structure in close resemblance with the X-ray structure.

These implications of the electrostatic stress hypothesis were investigated using the Asp91–Lys93–Asp96 complex, which includes the amino acids found by Warshel et al. to be the most important ones. The interaction energy of the amino acids was calculated quantum mechanically for the X-ray structure (1DQW) [19], and for the presently optimized TS and reactant structures. The interaction energies were obtained by subtracting the energy of the three individual amino acids from the energy of the total system. A 6-311+(2d,2p) basis set was used. For the X-ray structure hydrogen atoms have to be added, and the exact positions of these were determined in a B3LYP/d95 geometry optimization keeping the heavy atoms fixed.

Comparing the amino acid interaction energy in the optimized TS with that of the X-ray structure, the quantum mechanical calculations give a difference of only 2 kcal mol^{-1}, with a stronger interaction for the optimized TS. This result thus supports the hypothesis that the protein structure is optimized to stabilize the TS. On the other hand, comparing the interaction energy in the optimized reactant with that of the X-ray structure, the interaction energy of the optimized reactant is only 5 kcal mol^{-1} larger, indicating that the maximum electrostatic stress that could be introduced for the reactant is of this order of magnitude. This is much smaller than the effect of 14 (=38–24) kcal mol^{-1} obtained by Warshel et al. for the model having only Asp91, Lys93 and Asp96 charged. [31]

A difference between the present investigation and the calculations by Warshel et al. is that the interaction energy is here calculated quantum mechanically, while Warshel et al. used point charges to include the electrostatic effects. In the present study, the amino acids (including hydrogen atoms) were replaced by Mulliken point charges. Using Mulliken charges the interaction is found to be 4 kcal mol^{-1} weaker in the TS compared to the X-ray structure, to be compared to 2 kcal mol^{-1} stronger as was obtained from the quantum mechanical calculations. Furthermore, the difference between the optimized reactant and the X-ray structure is less than 1 kcal mol^{-1} if point charges are used, as compared to 5 kcal mol^{-1} in the quantum mechanical calculation. These results show that the Mulliken point charges do not reproduce the quantum mechanical values very well. However, the effects are of the same order of magnitude, and it can be concluded that electrostatic stress in the reactant of Model 3 may be underestimated by no more than 5 kcal mol^{-1} in the present calculations.

As mentioned above, Warshel et al. included charges to represent also a larger part of the enzyme. In order to investigate if charges outside the largest model used (Model 3) play a significant role, all aspartate, glutamate, histidine, lysine and arginine residues within 12 Å from the substrate in the *Saccharomyces cerevisiae* (yeast) enzyme were added as point charges to Model 3. The Mulliken atomic charge populations for these residues were calculated with B3LYP using the d95 basis set. Single point energy calculations (B3LYP/d95) were then made for the reactant and the TS with the additional amino acids modeled as atomic point charges at the same positions as they have relative to the phosphate group in the pdb-structure. In what is considered as the most likely protonation state (aspartates, glutamates and phosphate negative, histidines neutral, lysines and arginines positive) the reaction barrier decreased, but only by 3 kcal mol^{-1}, which is nearly insignificant in the present context. By varying the protonation states of these amino acids, effects on the reaction barrier from –3 to +4 kcal mol^{-1} were found. As a comparison, Warshel et al. found that different protonation states of this surrounding to the active site have a slightly larger effect on the energy barrier, making it decrease by up to 7 kcal mol^{-1}.

To summarize, possible deficiencies in the protein description in the present modeling of the direct protonation reaction mechanism, both with regard to electrostatic stress and geometric strain, have been investigated in this section. These estimates also give an upper limit to the catalyzing effects of some previous proposals for ODCase. The results are summarized in Table 2. For the electrostatic effects a maximum of about 5 kcal mol^{-1} could be estimated to be missing in the largest model calculations. For the effect of geometric strain, a maximal unrealistic value of 13 kcal mol^{-1} was calculated. It should be noted that since this latter value is obtained by quantum mechanical calculations it includes possible electrostatic effects. It is therefore concluded that the error in the calculated barrier due to the protein modeling is probably significantly lower than 10 kcal mol^{-1}, while the error as compared to experiment is about 20 kcal mol^{-1}.

The significant contribution of these calculations is that they indicate problems with all proposals related to the direct protonation mechanism. These mechanisms have too high barriers. Other significant effects have to be added, or other mechanistic proposals have to be investigated.

Table 2 Estimated stabilizing effects on the reaction barrier of ODCase for some selected proposals (from the section on electrostatic stress and geometric strain). Note that the effects are not in general additive

Proposal	Maximum effect (kcal mol^{-1})	Comment
Reactant destabilization	6	From calculation of proton affinity
Geometric strain	5	Completely rigid enzyme gives 13 kcal mol^{-1}
Preorganization energy	5	From interaction energies
Long range electrostatics	3	Point charges

The O2 mechanism

Since a low enough reaction barrier could not be found for a direct protonation reaction mechanism, the attention was switched to the previously suggested mechanism where the carbonyl oxygen O2 is protonated prior to decarboxylation, [13] see Fig. 3. Even before the X-ray determination of the structure, this mechanism was seriously criticized since quantum mechanical calculations on the substrate showed that protonation of O2 led to a very high barrier. [16, 17] The rejection of the O2 mechanism was further supported by the X-ray structure, which did not show any obvious proton donor in the vicinity of O2. The present renewed investigation of the O2 mechanism was motivated mainly by the failure to confirm the direct protonation mechanism and by the fact that the O4 mechanism is considered unlikely experimentally. The idea is to investigate if the detailed properties of the protein environment could affect the energetics of the O2 mechanism. This mechanism is further consistent with several early experiments, [3, 10, 12] and it can, for example, explain why there is no activity for the 2-thioOMP substrate, where O2 has been replaced by a sulfur. [3, 14] When the substrate with this substitution was modeled it was indeed found that the proton affinity of the O2 position decreased by 8 kcal mol^{-1} (small basis set), which would be enough to explain the loss of activity. However, this observed lack of activity, seemingly in favor of the O2 mechanism, has later been shown to be explained by a severely decreased binding affinity for the substrate. [15] Still, this explanation is not evidence against the O2 mechanism, which therefore remains a valid possibility.

Another feature that could be taken as support for the O2 mechanism is that the X-ray structures showed that the conserved Gln215 is located next to the O2 position. Gln215 also hydrogen bonds to the phosphate group, which has been shown to be important for proficient catalysis. [28] One possibility could be that the phosphate group loses a proton when it binds in to the positive group Arg235. The proton is then transferred to O2 via a hydrogen bonding chain involving Gln215. This scheme might fit into the kinetic analysis by Porter and Short [8] showing that the first step could be a complex function of ionizations (e.g. proton transfers) in the pyrimidinyl ring and the phosphate group.

The O2 mechanism is modeled in two steps. The first step is to protonate O2 and the second step is to decarboxylate the protonated substrate, see Fig. 7. In order to obtain the cost for protonating O2, a reasonable ground state first has to be defined. In line with Singleton et al., [17] the protonated carboxylate was chosen as the

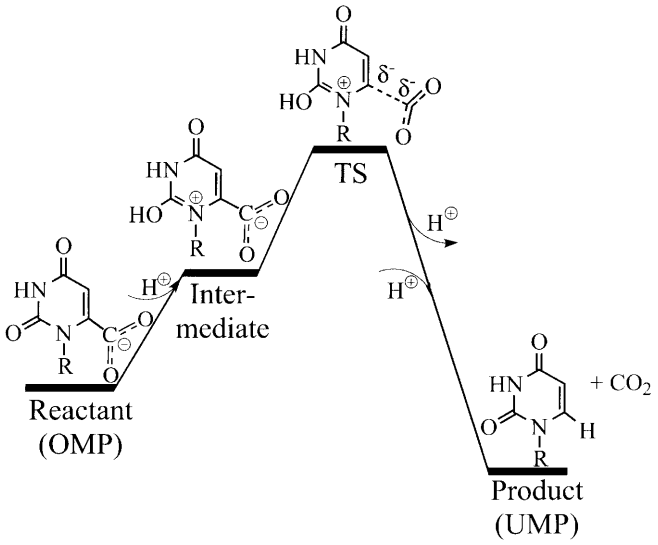

Fig. 7 Modeling of the O2 mechanism in two steps. The proton transfer from O2 to C6 has not been modeled

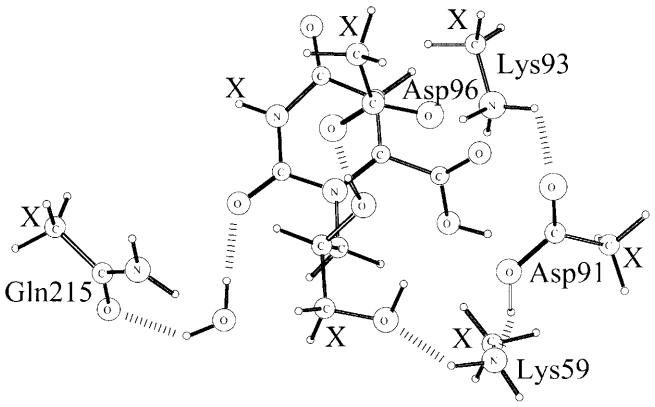

Fig. 8 Reactant structure (Model 8) used for calculating the cost of O2 protonation. Frozen atoms are marked with X

ground state, since this structure has the lowest energy in the model system. Modeling the substrate in the gas phase, Singleton et al. found a very high cost for protonating the carbonyl oxygen (42.1 kcal mol^{-1}), but a reasonable barrier for decarboxylation (8.4 kcal mol^{-1}). The total barrier is thus 50.5 kcal mol^{-1}. Using a homogenous medium with ε=4, the barrier for protonating O2 was found to decrease by 11 kcal mol^{-1}, to 31 kcal mol^{-1}, while the barrier for decarboxylation increased by a similar amount to 20 kcal mol^{-1}. The total barrier was thus still 51 kcal mol^{-1}. The inclusion of solvent effects stabilized the charge-separated carboxylate intermediate (species 2 in Fig. 7) but had a very limited effect on the total reaction. These compensating effects, making the specific value of the dielectric constant unimportant were discussed already by Beak and Siegel. [13] The decarboxylation transition state for the substrate (Model 6) was found at a bond distance of 2.4 Å. This transition state was localized by stepwise increasing the C–C bond, and adding entropy effects separately as described in [17] Thermal effects (including entropy) lower the barrier by approximately 3 kcal mol^{-1} at this point. A normal TS search cannot be successful since the energy without entropy effects increases monotonically with increasing bond length. To make the O2 mechanism plausible, the addition of amino acid residues from ODCase both must decrease the energy for protonating O2 and decrease the decarboxylation barrier.

The model is extended by including the four conserved amino acids Lys59, Asp91, Lys93 and Asp96. To keep the amino acid residues in positions resembling those in the X-ray structure, the outer carbon atoms on the amino acid models were frozen with respect to each other, to one atom in the orotidine ring (N3 hydrogen) and to the 3'C of the ribose (Model 7). This model gives a decarboxylation barrier of 12 kcal mol^{-1}. To calculate the barrier for this large model, it is assumed that the TS occurs at a C–C distance of 2.4 Å, as in Model 6. Previous calculations have indicated that the potential energy surface is rather flat in this region [17] and test calculations confirm this. To further save computational time, the large basis set used to calculate the reaction barrier for the O2 mechanism has been d95+(d,p) instead of d95+(2d,2p). No calculation of thermal effects through a Hessian was made for this large model since the frozen coordinates imply that the system is not at a true extremum. Instead, the thermal effects from Model 6 were used. The major entropy contribution should be in the release of CO_2 and that effect is already included in a small system. 12 kcal mol^{-1} is a quite low barrier compared to 20 kcal mol^{-1} obtained by treating the protein as a dielectric medium only. The lowering of the barrier for decarboxylation is probably due to the hydrogen bonding possibilities to two negatively charged aspartates for the positive lysine to compensate for the loss of contact with the carboxylate during decarboxylation. Since the proton affinity of O2 in this model is still low, the total reaction barrier is as high as 42 kcal mol^{-1}.

To improve the model at the O2 side, the conserved Gln215 is included. In one of the X-ray structures [20] water is present between Gln215 and O2. Since the proton affinity of O2 was found to increase if a water molecule is present at this position, it is included in the model in Fig. 8 (Model 8). For this model, the energy required to move a proton from carboxylate to O2 decreases from 31 kcal mol^{-1} in Model 6 (without any amino acids) to 7 kcal mol^{-1}. A major part of the effect arises from the stabilization of a proton at O2 by groups that are capable of forming strong hydrogen bonds.

To obtain the barrier for the whole process, the barrier of 12 kcal mol^{-1} for decarboxylation (obtained from Model 7), can be combined with the cost of 7 kcal mol^{-1} to move the proton to O2 (obtained from Model 8). This leads to an estimated energy barrier of 19 kcal mol^{-1}, which is in reasonable agreement with experimental results. However, if the calculations for the decarboxylation step is performed using the larger model in which the Gln215–H_2O is present at O2 (Model 8), the barrier for this step becomes 7 kcal mol^{-1} higher and the total

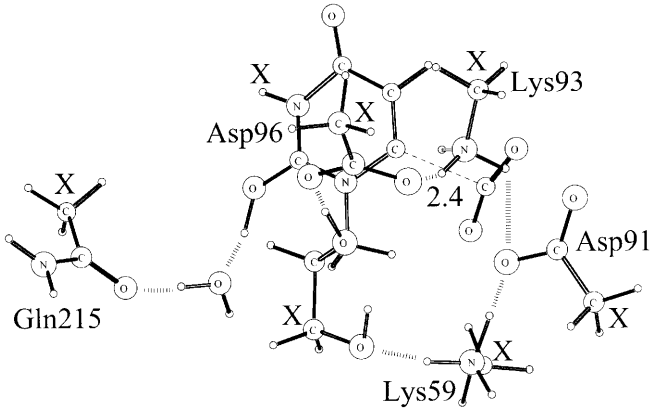

Fig. 9 TS for decarboxylation of an O2 protonated substrate (Model 8). The total barrier for decarboxylation is 26 kcal mol^{-1}. Completely frozen atoms are marked with X. The number 2.4 represents the frozen bond distance in Å

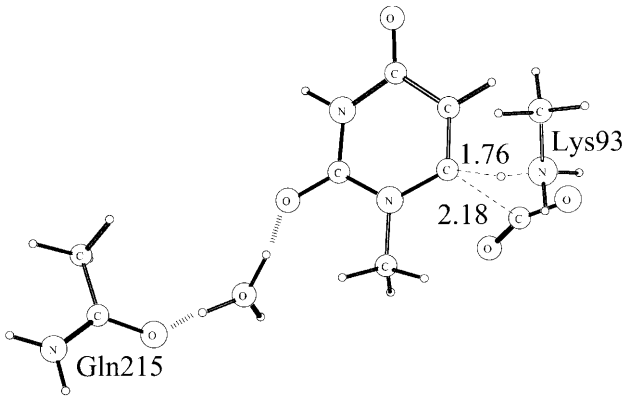

Fig. 10 TS for a concerted reaction where a proton is available at O2 to decrease the strength of the C–C bond (Model 9). Numbers represent bond distances in Å

barrier increases to 26 kcal mol^{-1} (Fig. 9), which is then significantly higher than the experimental value of 15 kcal mol^{-1}. This result shows that, the more stabilized the proton is at the O2 side, the less it participates in stabilization of the negative charge on C6 at the transition state for decarboxylation.

Furthermore, if the thermal properties are considered, experiments indicate that the entropic contribution increases the barrier by 4 kcal mol^{-1} [9]. This does not appear to be consistent with a mechanism with unconcerted release of CO_2 (as in the O2 mechanism), since the entropy contribution for this process decreases the barrier (by about 3 kcal mol^{-1}). A tighter TS complex should better explain the thermal data of the catalyzed reaction. Therefore a concerted reaction with Lys93 was attempted for a model where O2 is protonated. Since the O2 protonation decreases the energy to stretch the C–C bond, it might lower the barrier of a concerted reaction. Stretching of the C–C bond also increases the proton affinity of O2. However, when C6 becomes protonated by Lys93, the O2 proton must leave to avoid a positively charged product. Therefore the O2 proton must have a possibility to leave at the end of the reaction. A concerted TS where CO_2 and the O2 proton leave at the same time as Lys93 donates a proton to C6 might be a possibility. In a model with Lys93 and Gln215–H_2O at O2 (Model 9), no such TS could be found, but only a TS where the proton has already left O2 for the Gln215–H_2O complex. The calculated energy barrier for this reaction is 37 kcal mol^{-1} (Fig. 10), i.e. the same as for the model where O2 is not protonated, as discussed in the previous section on the direct protonation reaction mechanism.

In addition, the recently published Q215A mutation experiment, showing that the reaction proceeds at the same rate in the mutant, seems difficult to incorporate into a picture where O2 protonation is crucial. The mutation result is unexpected, since it has also been shown that O2 is important for substrate binding, and the only interaction between O2 and the enzyme is through Gln215. Possibly another group performs the same function in the mutated enzyme.

An alternative possibility to resolve the present disagreement with experiments might be to consider the suggestion that OMP binds in with the base rotated 180° around the glycosidic bond compared to the position of the inhibitors in the X-ray structures. [15] A mechanism starting from such a structure would suffer from the same general problem as the O2 mechanism, the low proton affinity of O2. Calculations on a simple model with a lysine at O2 shows that this residue does not protonate O2 when the C–C bond is extended. The energies for stretching the C–C bond are similar to the ones without enzyme residues (Model 6). This mechanism thus also suffers from a barrier which is much too high, at least in this small model.

In summary, the present results give a lower barrier for the O2 mechanism than for the direct protonation mechanisms. By adding five conserved amino acid residues, the barrier decreases by 25 kcal mol^{-1} (from 51 kcal mol^{-1} to 26 kcal mol^{-1}) but still does not reach agreement with experimental results. For the O2 mechanism there is thus a stabilizing effect from the conserved amino acids around the active site, while no such stabilization was found for the direct protonation mechanism. However, the computed barrier for the O2 mechanism is still about 11 kcal mol^{-1} higher than the experimental value. This might be due to inadequate modeling. It is known from experiments that the phosphate group has a large influence on k_{cat}. Mutations of other amino acids also decrease the reaction rate. The present model does not take these effects into account. As experimental data seem to favor a concerted mechanism, the most natural alternative at this stage seems to be a concerted mechanism with O2 protonated, but with a more accurate treatment of the phosphate group and the other conserved amino acids surrounding the substrate.

The O4 mechanism

The significant stabilization of the transition state in the ODCase reaction by protonation of one of the carbonyl oxygens is an important result reached here and which was also found previously. [16, 17] The previous calculations, performed on a model containing only the substrate, favored protonation of O4 by 16 kcal mol^{-1} compared to O2. If the four conserved amino acids close to the carboxylate group are included in the model (Model 10) a similar result is obtained. Another important result of the present study is that the enzyme residues close to O2 significantly increase its proton affinity, and if the different protein surroundings of the two carbonyl groups are taken into account the favorable energetics for protonation of O4 compared to O2 is removed.

On the basis of the X-ray structures, where Lys93 is far away from O4, Houk et al. have proposed a new version of their O4 protonation mechanism, where Lys93 protonates O4 mediated by a water molecule. [48] Such a mechanism was investigated in the present study and a barrier of 30 kcal mol^{-1} was obtained. Adding an aspartate between the water molecule and O4 (leading to Model 4b) gives a similar result (31 kcal mol^{-1}). The corresponding mechanism with a bridge to O2 (Model 4a) is shown in Fig. 6. In the optimized transition state for decarboxylation the proton still remains on Lys93. Thus, the suggested addition of a water molecule does not change the energetics significantly.

It can be concluded that the present results do not rule out the O4 protonation mechanism. Still, the O4 mechanism was not treated further in this study, mainly because it seems to be unlikely from experimental evidence as mentioned in the introduction.

Conclusions

The present theoretical study shows that several issues still have to be clarified before the catalytic proficiency of ODCase can be fully understood. In high level calculations including five conserved amino acids, the calculated barrier for decarboxylation, without protonation of O2 or O4, is 20 kcal mol^{-1} higher than the experimental result. Calculations using the coupled cluster G2MS method do not give any indications that the B3LYP method should overestimate the barrier. On the contrary, a slight underestimation is more likely. Effects of charged groups and electrostatic stress in the active site do not lower the barrier significantly (see Table 2). The direct protonation mechanism with Lys93 is therefore not supported by the present results, since this type of mechanism does not stabilize the TS sufficiently.

Significant stabilization of the TS has only been found when a carbonyl oxygen of the substrate is protonated, which is in line with previous studies. [16] The energy required to perform this protonation is significantly lower than previously obtained in the gas phase. [17] For a decarboxylation mechanism involving O2 protonation, the addition of five conserved amino acids decreases the barrier by 25 kcal mol^{-1}, but still does not reach agreement with experimental results. The calculations on the largest models show that O2 protonation is not disfavored compared to O4 protonation, which is in contrast to previous results from gas phase calculations. Involvement of O2 seems more likely since experimental results strongly suggest O2 rather than O4 protonation. [3, 14] There are also more interesting structural features near O2.

On the basis of the present results it can be concluded that a plausible reaction mechanism should involve proton transfer to O2 concerted with cleavage of the C–C bond, and after that proton transfer from O2 concerted with protonation of C6 by Lys93. At present it is not possible to adequately model such a mechanism, due to limitations in the size of the computational model. For this reason, the influences of the phosphate group [28] and the amino acids binding to this group [25] have so far not been investigated. To study the importance for k_{cat} of D37 and T100 as indicated by mutation experiments and the effect of the 2'OH group [26] also require larger models than presently afforded. An extension of the model system to include these amino acids and a larger part of the substrate might be done using QM/MM methods.

Supplementary material

Cartesian coordinates for the optimized structures of Model 1-10 are available in PDF format.

References

1. Lieberman I, Kornberg A, Simms ES (1955) J Biol Chem 21: 403–415
2. Radzicka A, Wolfenden R (1995) Science 267:90–92
3. Shostak K, Jones ME (1992) Biochemistry 31:12155–12161
4. Cui W, DeWitt JG, Miller SM, Wu W (1999) Biochem Biophys Res Commun 259:133–135
5. Miller BG, Smiley JA, Short SA, Wolfenden R (1999) J Biol Chem 274:23841–23843
6. Bell JB, Jones ME (1991) J Biol Chem 266:12662–12665
7. Yablonski MJ, Pasek DA, Han BD, Jones ME, Traut TW (1996) J Biol Chem 271:10704–10708
8. Porter DJT, Short SA (2000) Biochemistry 39:11788–11800
9. Wolfenden R, Snider M, Ridgway C, Miller B (1999) J Am Chem Soc 121:7419–7420
10. Smiley JA, Paneth P, O'Leary MH, Bell JB, Jones ME (1991) Biochemistry 30:6216–6223
11. Silverman RB, Groziak MP (1982) J Am Chem Soc 104: 6434–6439
12. Acheson SA, Bell JB, Jones ME, Wolfenden R (1990) Biochemistry 29:3198–3202
13. Beak P, Siegel B (1976) J Am Chem Soc 98:3601–3605
14. Smiley JA, Saleh L (1999) Bioorg Chem 27:297–306
15. Smiley JA, Hay KM, Levison BS (2001) Bioorg Chem 29: 96–106
16. Lee JK, Houk KN (1997) Science 276:942–945
17. Singleton DA, Merrigan SR, Kim BJ, Beak P, Phillips LM, Lee JK (2000) J Am Chem Soc 122:3296–3300
18. Appleby TC, Kinsland C, Begley TP, Ealick SE (2000) Proc Natl Acad Sci USA 97:2005–2010

19. Miller BG, Hassell AM, Wolfenden R, Milburn MV, Short SA (2000) Proc Natl Acad Sci USA 97:2011–2016
20. Wu N, Mo Y, Gao J, Pai EF (2000) Proc Natl Acad Sci USA 97:2017–2022
21. Harris P, Poulsen J-CN, Jensen KF, Larsen S (2000) Biochemistry 39:4217–4224 20
22. Smiley JA, Jones ME (1992) Biochemistry 31:12162–12168
23. Traut TW, Temple BRS (2000) J Biol Chem 275:28675–28681
24. Miller BG, Snider MJ, Wolfenden R, Short SA (2001) J Biol Chem 276:15174–15176
25. Miller BG, Snider MJ, Short SA, Wolfenden R (2000) Biochemistry 39:8113–8118
26. Miller BG, Butterfoss GL, Short SA, Wolfenden R (2001) Biochemistry 40:6227–6232
27. Miller BG, Traut TW, Wolfenden R (1998) J Am Chem Soc 120:2666–2667
28. Miller BG, Traut TW, Wolfenden R (1998) Bioorg Chem 26:283–288
29. Feng WY, Austin TJ, Chew F, Gronert S, Wu W (2000) Biochemistry 39:1778–1783
30. Warshel A, Florián J (1998) Proc Nat Acad Sci USA 95: 5950–5955
31. Warshel A, Štrajbl M, Villà J, Florián J (2000) Biochemistry 39:14728–14738
32. Ehrlich JI, Hwang C-C, Cook PF, Blanchard JS (1999) J Am Chem Soc 121:6966–6967
33. Rishavy MA, Cleland WW (2000) Biochemistry 39:4569–4575
34. Phillips LM, Lee JK (2001) J Am Chem Soc 123:12067–12073
35. Becke AD (1993) J Chem Phys 98:1372–1377
36. Becke AD (1993) J Chem Phys 98:5648–5652
37. Frisch MJ, Trucks GW, Schlegel HB, Scuseria GE, Robb MA, Cheeseman JR, Zakrzewski VG, Montgomery JA, Stratman RE, Burant JC, Dapprich S, Millam JM, Daniels AD, Kudin KN, Strain MC, Farkas O, Tomasi J, Barone V, Cossi M, Cammi R, Mennucci B, Pomelli C, Adamo C, Clifford S, Ochterski J, Petersson GA, Ay-ala PY, Cui Q, Morokuma K, Malick DK, Rabuck AD, Raghavachari K, Foresman JB, Cioslowski J, Ortiz JV, Baboul AG, Stefanov BB, Liu C, Liashenko A, Piskorz P, Komaromi, I, Gomperts R, Martin RL, Fox DJ, Keith T, Al-Laham MA, Peng CY, Nanayakkara A, Gonzalez C, Challacombe M, Gill PMW, Johnson BG, Chen W, Wong MW, Andres JL, Gonzales C, Head-Gordon M, Replogle ES, Pople JA (1998) Gaussian 98. Gaussian, Pittsburgh, Pa.
38. Dunning TH Jr, Hay PJ (1976) Gaussian basis sets for molecular calculations. In: Schaefer HF (ed) Methods of electronic structure theory, modern theoretical chemistry, vol 3. Plenum Press, New York, pp 1–28
39. Siegbahn PEM (1996) Electronic structure calculations for molecules containing transition metals. In: Prigogine I, Rice SA (eds) New methods in computational quantum mechanics, advances in chemical physics, vol XCIII. Wiley Interscience, New York, pp 333–387
40. Curtiss LA, Raghavachari K, Redfern RC, Pople JA (2000) J Chem Phys 112:7374–7383
41. Froese RDJ, Humbel S, Svensson M, Morokuma K (1997) J Phys Chem A 101:227–233
42. Klamt A, Schuurmann G (1993) J Chem Soc, Perkin Trans 2 5:799–805
43. Barone V, Cossi M (1998) J Phys Chem A 102:1995–2001
44. Warshel A, Florián J, Štrajbl M, Villà J (2001) ChemBioChem 2:109–111
45. Begley TP, Appleby TC, Ealick SE (2000) Curr Opin Struct Biol 10:711–718
46. Warshel A (1998) J Biol Chem 273:27035–27038
47. Villà J, Warshel A (2001) J Phys Chem B 105:7887–7907
48. Houk KN, Lee JK, Tantillo DJ, Bahmnanyar S, Hietbrink BN (2001) ChemBioChem 2:113–118